Shape fixity and shape recovery of polyurethane shape-memory polymer foams

H Tobushi[1]*, **D Shimada**[1], **S Hayashi**[2] and **M Endo**[3]
[1]Department of Mechanical Engineering, Aichi Institute of Technology, Toyota, Japan
[2]Nagoya Research and Development Center, Mitsubishi Heavy Industries Ltd., Nagoya, Japan
[3]Toshiba Ceramics Co. Ltd., Tokyo, Japan

Abstract: The thermomechanical properties of polyurethane shape memory polymer (SMP) foams were investigated experimentally. The results obtained can be summarized as follows. (1) By cooling the foam after compressive deformation at high temperature, stress decreases and the deformed shape is fixed. Stress decreases markedly in the region of temperature below the glass transition temperature T_g during the cooling process. (2) By heating the shape-fixed foam under no load, the original shape is recovered. Strain is recovered markedly at the temperature region in the vicinity of T_g. (3) The ratio of shape fixity is 100 per cent and that of shape recovery 98 per cent. Neither ratio depends on the number of cycles. (4) Recovery stress increases by heating under constraint of the fixed shape. Recovery stress is about 80 per cent of the applied maximum stress. Relaxed stress at high temperature is not recovered. (5) The shape deformed at high temperature is maintained for six months under no load at $T_g - 60\,\text{K}$ without depending on maximum strain, and the original shape is recovered by heating thereafter. (6) If the deformed shape is kept at high temperature, the original shape is not recovered. The factors influencing the shape irrecovery are the holding conditions of strain, temperature, and time.

Keywords: shape memory polymer, polyurethane, foam, shape fixity, shape recovery, recovery stress, glass transition, compression, cyclic deformation

NOTATION

a	material parameter
E	elastic modulus
E_g	value of E at T_g
N	number of cycles
R_f	rate of shape fixity
R_r	rate of shape recovery
t	time
t_c	holding time below T_g
t_r	stress-relaxation time above T_g
T_g	glass transition temperature
T_h	high temperature
T_l	low temperature
ε	compressive strain
$\dot{\varepsilon}$	strain rate
ε_{ir}	strain obtained after heating above T_g
ε_m	maximum compressive strain
ε_p	residual strain obtained by holding at high temperature
ε_u	strain obtained after unloading at low temperature
σ	compressive stress
σ_m	maximum compressive stress

1 INTRODUCTION

Shape memory polymer (SMP) is just one of the high-performance materials that have been developed and are now being used in practical applications [1–4]. Since the glass transition temperature, T_g, of polyurethane-series SMP can be set around room temperature and the characteristics of molecular motion differ above and below T_g, the mechanical properties differ markedly above and below T_g [5–7]. Shape fixity and shape recovery exist as a result of these differences in properties. Shape fixity and shape recovery properties are made use of in the fields of technology, medical treatment, aerospace engineering [8], and so on. Polyurethane SMP foams not only have these characteristics, but also energy absorption and heat insulating properties [9]. Because polyurethane SMP foams have these many good features, applications of the SMP foams are expected

L03202 © IMechE 2003

Proc. Instn Mech. Engrs Vol. 217 Part L: J. Materials: Design and Applications

to be diverse. In order to design SMP-foam elements in a rational names, it is important to evaluate the functional properties of the material.

In the present paper, in order to study the thermomechanical properties of polyurethane SMP foams, shape fixity, shape recovery, and recovery stress are investigated. By applying thermomechanical load in combination with loading–unloading and heating–cooling and by investigating shape fixity and shape recovery, it is found that the rates of shape fixity and shape recovery are higher than 98 per cent. By applying strain above T_g, followed by cooling under constant strain, stress diminishes. If the stress-diminished foam is heated by keeping the strain constant, recovery stress appears. A method for obtaining recovery stress effectively in applications is discussed. The conditions that affect shape recovery are also discussed.

2   MECHANISM OF SHAPE FIXITY AND SHAPE RECOVERY

The relationship between the storage elastic modulus and the temperature of SMP foam is shown in Fig. 1. The relationship was obtained from the dynamic mechanical test. The test was performed under compression. As can be seen from Fig. 1, the elastic modulus E varies markedly in the glass transition region. E is very low in the rubbery region above T_g and very high in the glassy region below T_g. SMP is composed of soft segments and hard segments [1, 5]. The micro-Brownian motion of soft segments of SMP is active above T_g. Therefore E is low above T_g; SMP therefore deforms easily and the original shape is recovered during unloading. The micro-Brownian motion of soft segments is frozen below T_g. Therefore E is high below T_g and SMP is hard to deform.

Based on the abovementioned properties, if SMP foam that has been deformed above T_g is cooled below T_g, the deformed shape is fixed. This property is called shape fixity. In the state below T_g, because SMP foam is hard, it can carry large load. Following this cooling process, if the shape-fixed SMP foam is heated to above T_g, it regains its original
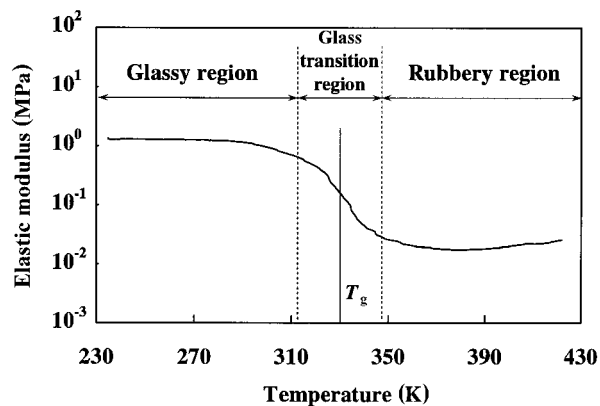
shape. This property is called shape recovery. As mentioned above, SMP foam changes shape when heated and retains its new shape when cooled. If the material is then reheated, it remembers its original shape and returns to it. These phenomena form the basic mechanism of shape fixity and shape recovery of SMP foam.

3   EXPERIMENTAL METHOD

3.1   Materials and specimens

The material used in the experiment was polyurethane SMP foam of the polyether polyol series (Diary MF 5520: produced by Mitsubishi Heavy Industries, Ltd.). The foam was made by chemical foaming. The expansion ratio was about 14 and the structure was open cell. The foam was produced as slabstock. The specimen was a column with height 20 mm and diameter 20 mm. The glass transition temperature T_g was 328 K.

3.2   Experimental apparatus

A shape-memory material testing machine [7] was used for the experiment. The testing machine was composed of the loading system (to apply loading–unloading cycles) and the temperature-controlling system (to perform heating–cooling cycles). The temperature of the specimen was measured using a thermocouple of diameter 0.1 mm, which was in contact with the side of the foam. With respect to the constant heating–cooling rate, temperature was measured at three positions on the side, in the central part, and at the bottom of the specimen. It was confirmed that temperatures at each position were almost equal. Load and displacement were measured using a loadcell and displacement of a crosshead, respectively. A Teflon® sheet was placed between the specimen and a compression plate, resulting in small shearing resistance on the surface of contact. The specimen was compressed uniformly with constant Poisson's ratio along the axial direction of compression without expanding to a barreled shape. This is confirmed by the photographs of SMP foam under compression shown in Ref. 10.

3.3   Experimental procedures

In order to investigate the thermomechanical properties, four types of compression test were carried out, as described in the following. The heating–cooling rate was 5 K/min in each test.

3.3.1   Thermomechanical test

The three-dimensional stress–strain–temperature diagram in the thermomechanical test is presented in Fig. 2. At first, maximum compressive strain $-\varepsilon_m$ was applied at high temperature $T_h = T_g + 30$ K ①. Maintaining $-\varepsilon_m$, the specimen was cooled to low temperature $T_1 = T_g - 30$ K. Note that stress is reduced to zero at this stage ②. It was held at T_1 under the no-load condition for 10 min ③,
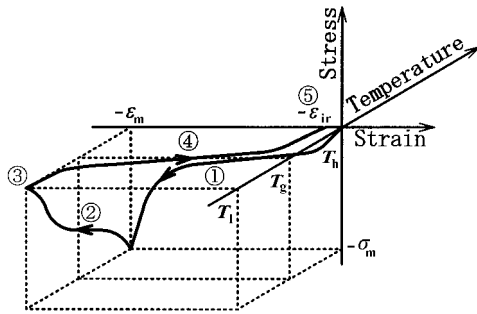

Fig. 1   Relationship between elastic modulus and temperature

Fig. 2 Three-dimensional stress–strain–temperature diagram showing the loading path in the thermomechanical compression test

Fig. 3 Three-dimensional stress–strain–temperature diagram showing the loading path in the recovery stress test

then heated up to T_h under the no-load condition ④. It was then held at T_h for 10 min ⑤. Thermomechanical paths ① to ⑤ were repeated 10 times. The strain rate $\dot{\varepsilon}$ was 25 per cent/min. In the experiment to investigate the influence of maximum strain on shape fixity and shape recovery, values of ε_m were 75, 78, and 85 per cent.

3.3.2 Recovery-stress test

The three-dimensional stress–strain–temperature diagram in the recovery-stress test is shown in Fig. 3. At first, maximum compressive stress $-\sigma_m$ was applied at T_h ①. Maintaining the compressive strain $-\varepsilon_m$ at the maximum stress point, the specimen was cooled down to T_l ②. Note that stress is reduced to zero at this stage ③. It was then held at T_l under the no-load condition for 10 min ④, then heated to T_h by maintaining the strain $-\varepsilon_m$ ⑤. Finally, it was held at T_h for 10 min.

3.3.3 Aging test held at low temperature

The experimental procedure in the aging test held at low temperature is schematically shown in Fig. 4. At first, maximum compressive strain $\varepsilon_m = 90$ per cent was applied at $T_g + 30$ K using the testing machine ①. The compressed shape was restricted by using two compression plates and was held at low temperature $T_g - 60$ K for 24 hours
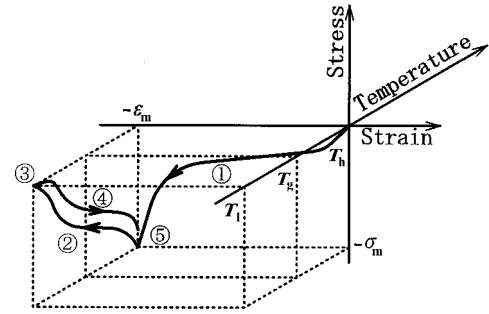
②. After 24 hours, the holding attachment was removed and the specimen was held again at $T_g - 60$ K under no load ③. After the prescribed holding time t_c at low temperature, height of the specimen was measured and the rate of shape fixity R_f was obtained ④. After heating under no load, the height of the specimen was measured and the rate of shape recovery R_r was obtained ⑤. The strain rate $\dot{\varepsilon}$ during loading to $-\varepsilon_m$ was 25 per cent/min. The holding times t_c at low temperature were 2, 6, 18, 57, and 180 days.

In order to observe the influence of maximum strain on shape recovery, the following test was carried out. At first, various maximum strains $-\varepsilon_m$ were applied at $T_g + 30$ K. After holding at $T_g - 60$ K for 24 hours, the shape was recovered by heating and the rate of shape recovery was obtained.

3.3.4 New-shape forming test held at high temperature

The experimental procedure in the new-shape forming test held at high temperature is schematically shown in Fig. 5. At first, maximum compressive strain $-\varepsilon_m$ was applied at $T_g + 30$ K using the testing machine ①. The specimen was compressed by using two compression plates in order to keep $-\varepsilon_m$ constant, and the compressed specimen was held at a certain constant temperature in a furnace ②. After the prescribed holding time, the specimen was taken out
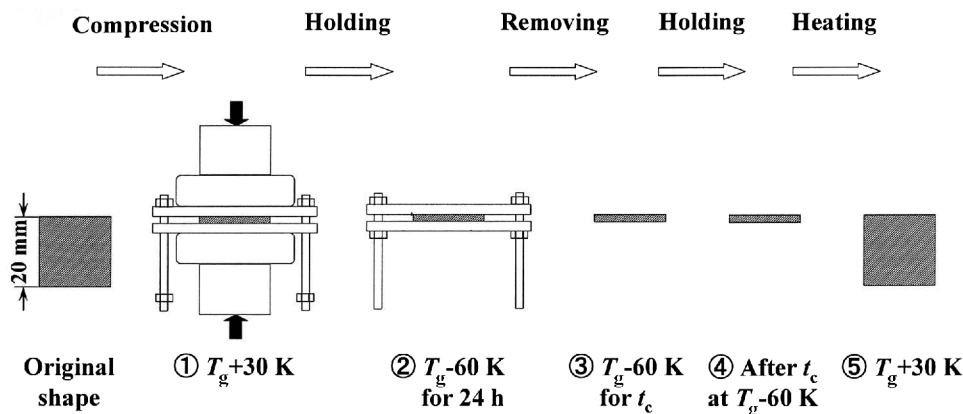

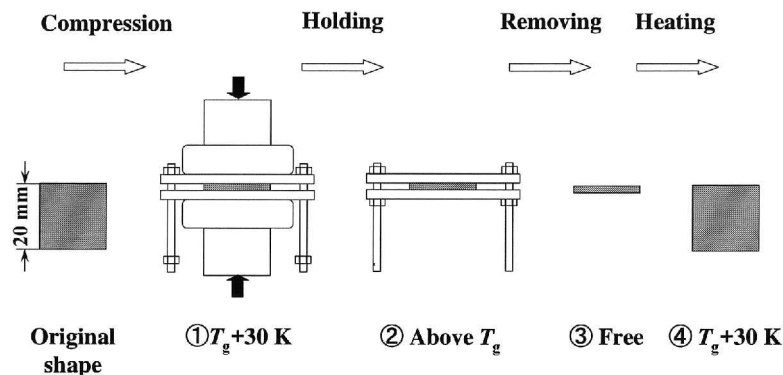**Fig. 4** Experimental procedure of the aging test held at low temperature

Fig. 5   Experimental procedure of the new-shape forming test held at high temperature

from the furnace and the holding attachment was removed ③. The shape of the specimen was recovered by heating at $T_g + 30$ K and the height of the specimen was measured ④. By this procedure, residual strain ε_p at $T_g + 30$ K was obtained.

Strain rate $\dot{\varepsilon}$ was 10 per cent/min in the loading process to apply $-\varepsilon_m$. Maximum strains ε_m were 50, 70, and 90 per cent. The holding temperatures were T_g, $T_g + 30$ K, and $T_g + 60$ K. The holding times in the furnace were 2, 4, 8, 16, and 24 h.

4   RESULTS AND DISCUSSION

In dealing with the experimental data, stress and strain were treated in terms of nominal stress and nominal strain, respectively. Strain was calculated based on the initial length of 20 mm even in the process of shape recovery. The symbols ① to ⑤ used in the figures showing the experimental results correspond to the loading paths shown in Figs 2 and 3, while N denotes the number of cycles.

4.1   Shape fixity and shape recovery

Rate of shape fixity R_f and rate of shape recovery R_r were defined by the following equations.

$$R_f = \frac{\varepsilon_u}{\varepsilon_m} \times 100 \tag{1}$$

$$R_r = \frac{\varepsilon_m - \varepsilon_{ir}}{\varepsilon_m} \times 100 \tag{2}$$

where $-\varepsilon_u$ and $-\varepsilon_{ir}$ represent the strain obtained after holding the no-load condition below T_g and the strain obtained after holding the no-load condition above T_g, that is, irrecoverable strain, respectively.

4.1.1   Stress–strain relationship

The stress–strain curves obtained by the thermomechanical test for $\varepsilon_m = 78$ per cent are shown in Fig. 6. As can be seen,

yielding occurs in the vicinity of a strain of 10 per cent, a stress plateau appears thereafter until a strain of 60 per cent, and the slope of the curve becomes steep above a strain of 60 per cent. In the region of the stress plateau for strain from 10 to 60 per cent, buckling of cells propagates in the axial direction of compression. In the upswing region above a strain of 60 per cent, the material is compressed uniformly and deformation resistance increases. With respect to the cyclic properties in the loading process ①, stress decreases slightly in $N = 2$ and decreases gradually thereafter. In the cooling process ②, stress disappears perfectly at temperature T_l. Therefore ε_m is maintained and $\varepsilon_u = \varepsilon_m$, resulting in a rate of shape fixity R_f of 100 per cent. In these processes, the influence of friction at both end surfaces of the specimen on the deformation is negligibly small. This is confirmed by photographs of SMP foam under compression [**10**], in which it can be seen that the foam is compressed uniformly in the axial direction and therefore expands uniformly in the lateral direction at all positions of the vertical axis.

4.1.2   Stress–temperature relationship

The stress–temperature curves obtained by the thermomechanical test are shown in Fig. 7. As can be seen, stress decreases in the cooling process ②. Just after the start of
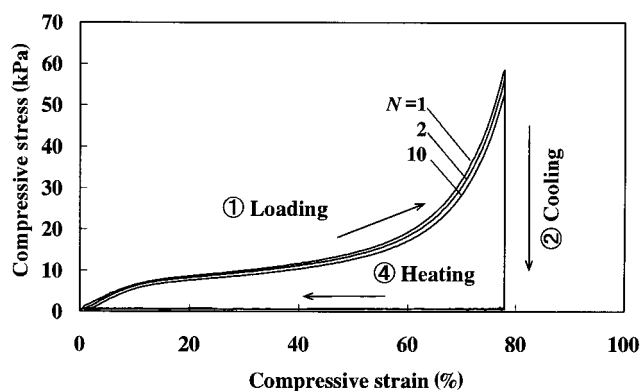

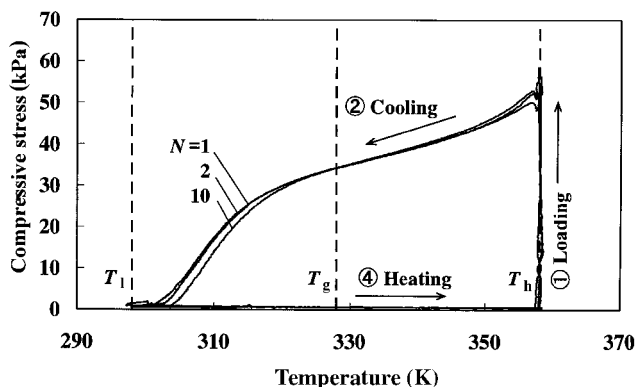**Fig. 6**   Stress–strain curves in the thermomechanical test

Fig. 7 Stress–temperature curves in the thermomechanical test

Fig. 9 Stress–temperature curves for various maximum strains

cooling, stress decreases due to stress relaxation at high temperature. In the middle stage of the process ②, stress decreases due to thermal contraction by cooling. Because a crosshead of the testing machine is held constant during the process ② and the compressed SMP foam contracts thermally, stress decreases. In the latter stage of the process ②, the level of decrease in stress is large. This is because the modulus of elasticity of SMP is quite large at temperatures below T_g as observed in Fig. 1, and the rate of variation in thermal stress increases due to thermal contraction based on decrease in temperature. As a result, the slope of the curve becomes steep at low temperature. The stress–temperature curves do not change under repetition.

4.1.3 Strain–temperature relationship

The strain–temperature curves obtained by the thermomechanical test are shown in Fig. 8. As can be seen, in the heating process ④, strain is recovered significantly in the vicinity of T_g. Because the micro-Brownian motion of soft segments of SMP is frozen in the glassy region at temperatures below T_g, strain maintains ε_m. Since the micro-Brownian motion becomes active if the material is heated up to temperatures in the vicinity of T_g, strain is recovered. The strain–temperature curves do not change under repetition. Irrecoverable strain remaining after heating is small
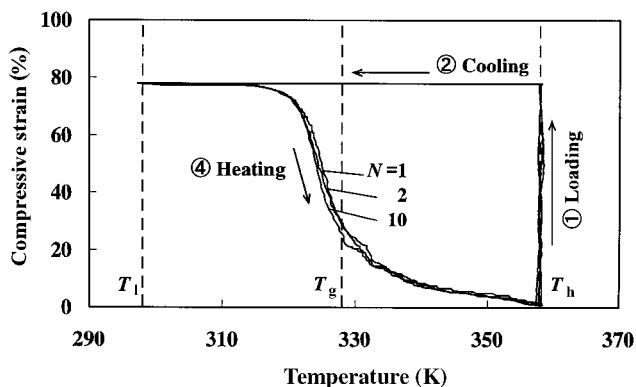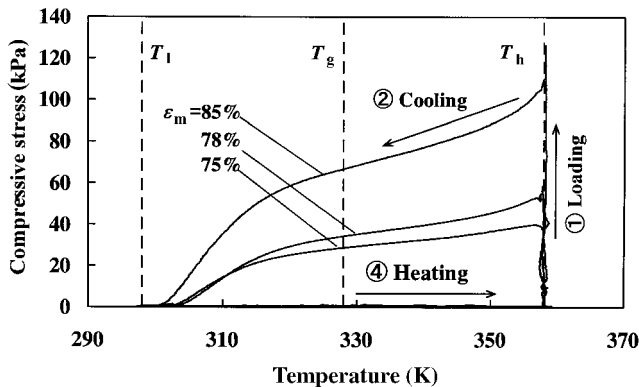
without depending on the number of cycles, and the rate of shape recovery R_r is 99 per cent.

4.1.4 Dependence on maximum strain

The stress-temperature curves in $N = 1$ obtained by the thermomechanical test for various maximum strains ε_m are shown in Fig. 9. As can be seen, the larger the ε_m, the more steep the slope of the curve just after the start of the cooling process ②. This occurs due to the fact that stress relaxation appears markedly for large ε_m. Except for the difference in stress level corresponding to the difference in ε_m, the stress–temperature relationships are almost similar.

The strain–temperature curves in $N = 1$ obtained by the thermomechanical test for various maximum strains ε_m are shown in Fig. 10. As can be seen, strain is recovered at temperatures in the vicinity of T_g for each ε_m in the heating process ④. The temperature at which strain is recovered markedly moves to lower temperature as ε_m increases. If ε_m is large, internal stress induced in the material increases. The internal stress acts to enable strain to be recovered. Therefore, since the action of internal stress is added to the
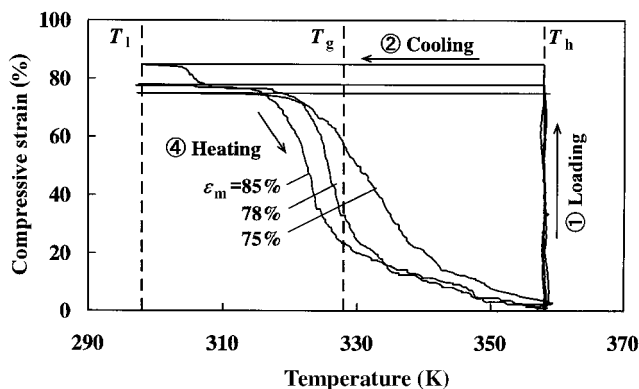

Fig. 8 Strain–temperature curves in the thermomechanical test
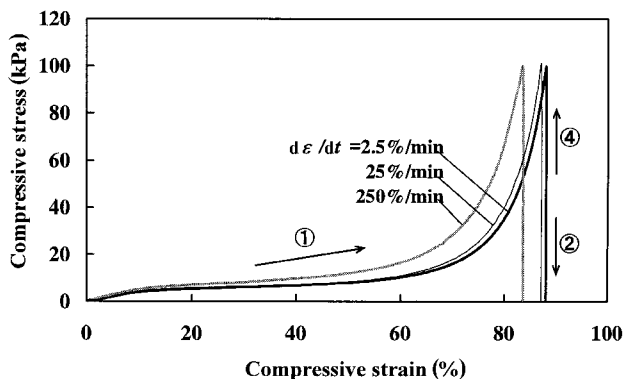

Fig. 10 Strain–temperature curves for various maximum strains

Fig. 11　Stress–strain curves in the recovery-stress test

Fig. 13　Stress–time curves in the recovery-stress test with various stress-relaxation times t_r

micro-Brownian motion due to thermal energy in the case of larger ε_m, strain is recovered at lower temperature.

4.2　Recovery stress

4.2.1　Dependence on strain rate

The recovery stress test for various strain rates $\dot{\varepsilon}$ under a constant maximum compressive stress $\sigma_m = 100\,\text{kPa}$ was carried out. The stress–strain curves and stress–temperature curves obtained by the test are shown in Figs 11 and 12, respectively. As can be seen in Fig. 11, the smaller the $\dot{\varepsilon}$ in the loading process ①, the smaller the deformation resistance and the larger the strain at the point of maximum stress. Figure 12 shows that the smaller the $\dot{\varepsilon}$, the larger the recovery stress obtained in the heating process ④. This occurs due to the fact that the amount of stress relaxation just after the start of cooling is slight if $\dot{\varepsilon}$ is small. If $\dot{\varepsilon}$ is small, the SMP foam is compressed slowly for a long time in the loading process ①, it becomes dense, and large compressive strain appears. As a result, stress relaxation is small. The temperature at which stress increases markedly in the heating process ④ is higher by about 10 K than that at which stress decreases markedly in the cooling process ②. This behaviour occurs due to the fact that, although the micro-Brownian motion of soft segments of SMP is frozen
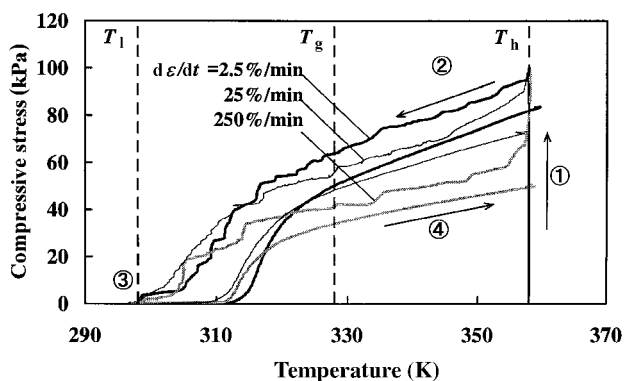
at low temperature and the molecular chain cannot move, the micro-Brownian motion becomes active by heating up to the vicinity of T_g and recovery stress appears gradually with an increase in temperature.

The relationship between stress–relaxation time and recovery stress was investigated. In the experiment, at first, maximum compressive stress $\sigma_m = 100\,\text{kPa}$ was applied at strain rate $\dot{\varepsilon} = 2.5$ per cent/min in the loading process ①. Maximum strain was held before the cooling process ②. The holding times t_r above T_g were 0, 60, and 180 min. Following stress relaxation, the recovery stress test with processes ② to ⑤ was performed. The stress–time curves and stress–temperature curves obtained by the test are shown in Figs 13 and 14, respectively. In Fig. 14, stress at the end of the process ⑤ is expressed by symbols ● in the case of $t_r = 60$ and 180 min. As can be seen in these figures, the stresses at $t_r = 60\,\text{min}$ and 180 min before cooling are almost recovered by heating, respectively. This means that the stress decreased by stress relaxation at T_h cannot be obtained as recovery stress by heating. Therefore, if recovery stress is used in applications, large recovery stress can be obtained by loading at low strain rate followed by cooling at high cooling rate. It should be noted that, in the case of loading at high strain rate, stress relaxation is large, resulting in small recovery stress.
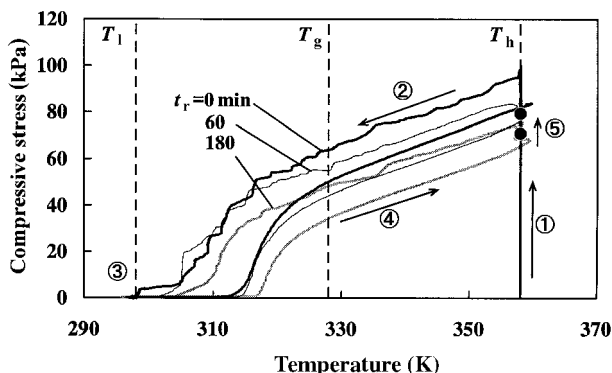

Fig. 12　Stress–temperature curves in the recovery-stress test

Fig. 14　Stress–temperature curves in the recovery-stress test with various stress-relaxation times t_r
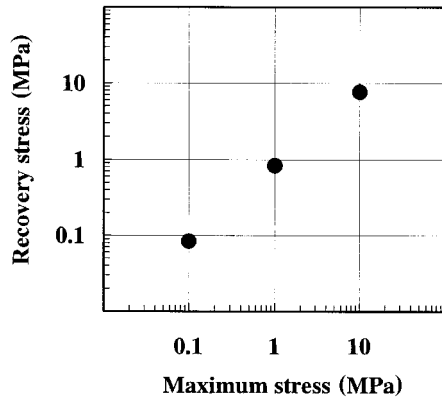
Fig. 15 Relationship between recovery stress and maximum stress

4.2.2 Dependence on maximum stress

The recovery stress test at $\dot{\varepsilon} = 2.5$ per cent/min in the loading process ① for various maximum compressive stresses σ_m was performed. In order to use a large restoring force or driving force in applications of SMP foam elements, the values of 100 kPa, 1 MPa, and 10 MPa were selected for σ_m. The relationship between the obtained recovery stress and the applied maximum stress is shown in Fig. 15. As can be seen, recovery stress is proportional to applied maximum stress. Recovery stress is about 80 per cent of the applied stress. In the case of recovery stress for SMP sheet and film under tension obtained by heating under constant strain, recovery stress is about 50 per cent of the applied stress [**11**]. Therefore, it must be a very effective method to obtain recovery stress by compressing SMP foam. Because a large change in volume can be obtained for SMP foam elements, they can be applied to the easily portable energy sources to use recovery stress.

4.3 Aging by holding at low temperature

The dependences of a rate of shape fixity R_f and a rate of shape recovery R_r on the holding time t_c, as obtained by the aging test held below T_g for maximum compressive strain $\varepsilon_m = 90$ per cent, are shown in Figs 16 and 17, respectively.
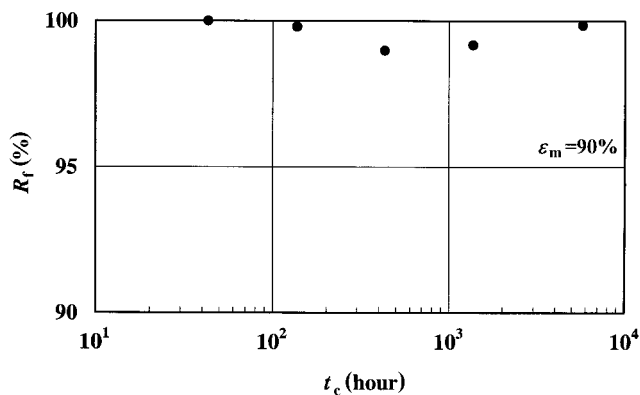

Fig. 16 Relationship between rate of shape fixity R_f and holding time t_c at $T_g - 60$ K
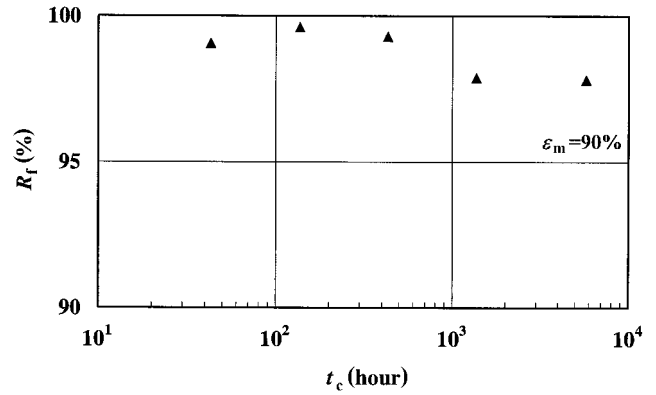

Fig. 17 Relationship between rate of shape recovery R_r and holding time t_c at $T_g - 60$ K

The relationship between a rate of shape recovery R_r and maximum strain ε_m obtained by the test for various ε_m holding for 24 hours at $T_g - 60$ K is shown in Fig. 18.

As can be seen in Fig. 16, a rate of shape fixity R_f is larger than 99 per cent even after more than 1000 hours. Although some quantities of shape are not fixed, these values are small enough. Therefore, the deformed shape can be fixed if it is held below $T_g - 60$ K. As can be seen in Fig. 17, a rate of shape recovery R_r is larger than 98 per cent without depending on the holding time. The small irrecoverable part may appear due to a decoupling imperfect molecular chain, collapse of cell, and reorientation of the molecular chain. As can be seen in Fig. 18, the fixed shape is almost recovered without depending on ε_m.

It is ascertained that a rate of shape fixity and a rate of shape recovery by holding the shape below T_g are greater than 98 per cent without dependence on the holding time and maximum strain, therefore resulting in good performance.

4.4 New-shape forming by holding at high temperature

In the process of the present study, it was found that if SMP foam was deformed and the deformed shape was held for a longer time at temperatures above T_g, irrecoverable
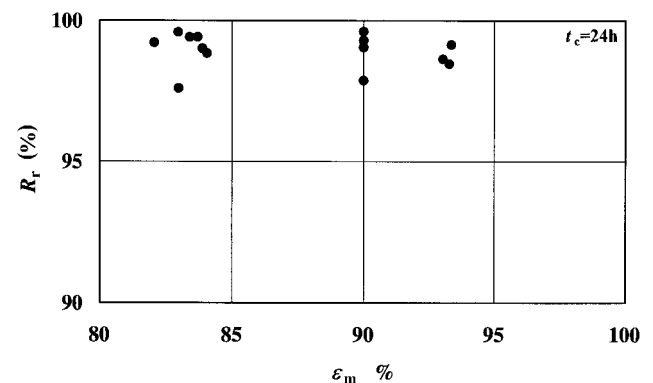

Fig. 18 Relationship between rate of shape recovery R_r and maximum strain ε_m held at $T_g - 60$ K for 24 h

deformation appeared. That is, it was found that the deformed shape was fixed. This phenomenon is called new-shape forming or secondary-shape forming. In order to investigate the phenomenon, the new-shape forming test in which the deformed shape was held above T_g for a certain time was carried out. The relationship between ratio $\varepsilon_p/\varepsilon_m$ of residual strain ε_p to maximum strain ε_m and the holding time obtained by the test is shown in Fig. 19. If the ratio is zero, new-shape forming does not appear. If the ratio is unity, ε_m remains intact. Therefore, $\varepsilon_p/\varepsilon_m$ expresses a rate of new-shape forming or a rate of irrecovery.

As can be seen in Fig. 19, ε_p occurs slightly at holding temperature T_g. This ε_p may occur due to the fact that weak cells in SMP foam collapse and the initial shape is not recovered. On the other hand, ε_m remains almost as ε_p at holding temperatures of $T_g + 60$ K. The reason why ε_p occurs is not a result of cell collapse but is due to new-shape forming. Therefore, if strain is kept above T_g, new-shape forming may appear easily. In the case of a holding temperature of $T_g + 30$ K, ε_p increases in proportion to the holding time. Therefore, new-shape forming appears easily if the material is held above T_g for a long time. In the case of $T_g + 60$ K, ε_p is large for large ε_m. From these results, it is ascertained that the factors to affect new-shape forming are the holding strain, temperature, and time. The cause of new-shape forming can be considered as follows. In the region of temperature above T_g, thermal motion of the molecular chain (micro-Brownian motion) is active and therefore reorientation of the molecular chain occurs when holding large strain for a long time. In order to avoid new-shape forming for the deformed SMP foam, it is important to keep the foam under the appropriate condition by considering these factors. One of the methods to prevent new-shape forming is to keep the foam below T_g. In the region of temperature below T_g, new-shape forming does not appear and both the rate of shape fixity and that of shape recovery are high. Therefore, holding at low temperature must be effective for applications of SMP foam elements.
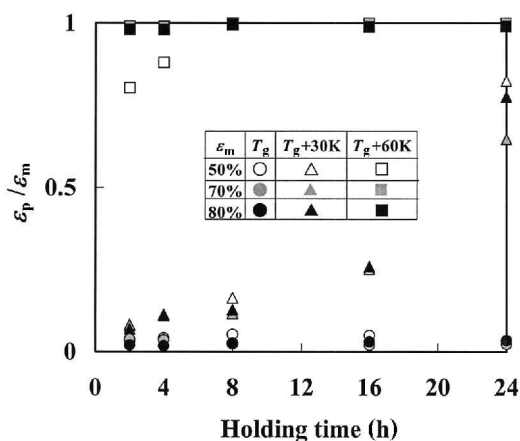

Fig. 19 Relationship between irrecovery ratio $\varepsilon_p/\varepsilon_m$ and holding time for various holding temperatures and maximum strains

5 MODELING OF THERMOMECHANICAL PROPERTIES OF SMP FOAM

The theoretical model to express the thermomechanical properties of SMP was developed based on linear and nonlinear viscoelastic theory [7, 11]. As shown in Fig. 1, the elastic modulus E varies markedly depending on temperature T in the glass transition region. This property can be expressed by the following equation:

$$E = E_g \exp\left[a\left(\frac{T_g}{T} - 1\right) \right] \tag{3}$$

where E_g is the value of E at $T = T_g$ and a is a material parameter. The exponential function (3) is similar to the equation for viscosity that was derived theoretically by Eyring and empirically by Arrhenius. In the model, other parameters are expressed by similar exponential functions of temperature. In the model, irrecoverable strain, which is composed of a time-dependent part and a time-independent part, is also considered.

In the case of SMP foam, as observed from the stress–strain curve shown in Fig. 6, the linear elastic region appears in the initial stage, the stress plateau region in the yielding stage, and the upswing region in the final stage. Although the strain appearing in the stress plateau region remains after unloading below T_g, the residual strain is recovered by heating above T_g. Therefore it is necessary to take account of these properties in the modeling of SMP foam. Furthermore, as observed in Fig. 12, stress is reduced to zero during cooling under constant strain and increases again during heating. These variations in stress appear based not only on the glass transition but also the thermal expansion and contraction. The deformation properties of SMP foam also depend strongly on the porosity of the foam [9].

In the modeling of the thermomechanical properties of SMP foam, as mentioned above, it is necessary to combine the model which expresses the thermomechanical properties of SMP and that which expresses the stress plateau due to buckling of cells and the upswing behaviour of the stress–strain curve due to densification of the foam. The modeling will be discussed in a subsequent paper.

6 CONCLUSIONS

Applying various thermomechanical loadings to polyurethane-SMP foams, thermomechanical properties of the material were investigated. The results obtained can be summarized as follows.

1. If the SMP foam deformed above T_g is cooled to below T_g, stress diminishes and the deformed shape is fixed. In the cooling process, stress decreases markedly below T_g.

2. If the SMP foam fixed at the deformed shape is heated under no load, shape is recovered. In the heating process, strain is recovered markedly in the vicinity of T_g.

3. The rate of shape fixity and that of shape recovery are 100 and 99 per cent, respectively. Both rates do not depend on the number of cycles.

4. If the SMP foam deformed above T_g followed by cooling is heated while holding the deformed shape, recovery stress appears. The recovery stress is about 80 per cent of the applied stress. If stress relaxation appears before cooling, the relaxed stress cannot be restored.

5. If the SMP foam is compressed above T_g followed by holding at $T_g - 60\,K$, the deformed shape is fixed even if the material is kept under no load for six months. The fixed shape is recovered by heating thereafter. Both the rates of shape fixity and shape recovery are larger than 98 per cent, and do not depend on holding time and maximum strain.

6. If the deformed SMP foam is held above T_g, new-shape forming appears. The factors affecting new-shape forming are holding strain, temperature, and time.

ACKNOWLEDGEMENTS

REFERENCES

1 Hayashi, S. Properties and applications of polyurethane series shape memory polymer. *Int. Progr. Urethanes*, 1993, **6**, 90–115.

2 Hayashi, S., Ishikawa, N. and **Jiordano, C.** High moisture permeability polyurethane for textile applications. *J. Coated Fab.*, 1993, **23**, 74–83.

3 Irie, M. Shape memory polymers. In Otsuka, K. and Wayman, C. M, Eds., *Shape Memory Materials*, 1998, pp. 203–219 (Cambridge University Press, Cambridge).

4 Liang, C., Rogers, C. A. and **Malafeew, E.** Preliminary investigation on shape memory polymers and their hybrid composites. *Smart Struct. Mater.*, 1991, **AD-Vol.24/AMD-Vol.123**, 97–105.

5 Takahashi, T., Hayashi, N. and **Hayashi, S.** Structure and properties of shape-memory polyurethane block copolymers. *J. Appl. Polym. Sci.*, 1996, **60**, 1061–1069.

6 Tobushi, H., Hayashi, T., Ito, N., Hayshi, S. and **Yamada, E.** Shape fixity and shape recovery in a film of shape memory polymer of polyurethane series. *J. Intell. Mater. Syst. & Struct.*, 1998, **9**, 127–136.

7 Tobushi, H., Okumura, K., Hayashi, S. and **Ito, N.** Thermo-mechanical constitutive model of shape memory polymer. *Mech. Mater.*, 2001, **33**, 545–554.

8 Ishizawa, J., Imagawa, K., Yoshikawa, J., Hayashi, S. and **Miwa, N.** Research on applicability of shape memory polymers (SMPs) to inflatable and deployable space structures. *Proc. 7th Japan Int. SAMPE Symposium & Exbn.*, 2001, pp. 295–298.

9 Gibson, L. J. and **Ashby, M. F.** Cellular Solids, Structure and Properties, 2nd ed., 1997, pp. 309–344 (Cambridge University Press, Cambridge).

10 Tobushi, H., Okumura, K., Endo, M. and **Hayashi, S.** Thermomechanical properties of polyurethane-shape memory polymer foam. *J. Intell. Mater. Syst. & Struct.*, 2001, **12**, 283–287.

11 Tobushi, H., Hashimoto, T., Hayashi, S. and **Yamada, E.** Thermomechanical constitutive modeling in shape memory polymer of polyurethane series. *J. Intell. Mater. Syst. & Struct.*, 1997, **8**, 711–718.